sensors

MDPI

Communication

Gas Sensor Based On Lossy Mode Resonances by means of thin Graphene oxide films fabricated onto planar coverslips

Ignacio Vitoria[1,2*], Elieser E. Gallego[1,3], Sonia Melendi-Espina[4], Miguel Hernaez[4], Carlos Ruiz Zamarreño[1,2], Ignacio R. Matías[1,2]

[1] Electrical, Electronic and Communications Engineering Department in the Public University of Navarre, Pamplona, 310016 Spain
[2] Institute of Smart Cities, Jeronimo de Ayanz Building, 31006 Pamplona (NA), Spain
[3] Telecommunications and Electronic Department , University of Pinar del Río, Pinar del Río, 20100, Cuba
[4] School of Engineering. University of East Anglia (UEA), Norwich Research Park, Norwich NR4 7TJ, UK
* Correspondence: ignacio.vitoria@unavarra.es

Abstract: The use of planar waveguides has recently shown great success in the field of optical sensors based on the Lossy Mode Resonance (LMR) phenomenon. Graphene Oxide (GO) properties have been widely exploited in various sectors of science and technology with promising results for gas sensing applications. This work combines both, the LMR-based sensing technology on planar waveguides and the use of a GO thin film as sensitive coating to monitor ethanol, water and acetone. Experimental results on the fabrication and performance of the sensor are presented. Obtained results showed a sensitivity of 3.1, 2.0, and 0.6 pm/ppm for ethanol, water and acetone respectively with a linearity factor R2 >0.95 in all cases.

Keywords: Gas sensor, Graphene Oxide, Lossy Mode Resonance, Optical fiber sensor

Citation: To be added by editorial staff during production.

Academic Editor: Firstname Lastname

Received: date
Accepted: date
Published: date

1. Introduction

The demand of new gas sensors has been increased in the last few years associated to the development of smart cities or industry 4.0, which require the collection of significant amounts of data through multiple sensors [1,2]. For example, the monitoring of air quality in cities is crucial, as strict regulations impose limits to the concentration of several gases either outdoor or indoor [1]. Air quality is a key and very relevant aspect in the development and improvement of smart, highly efficient, and citizen-oriented cities. In fact, the European Commission is currently financing a number of projects around these lines [3]. Gas sensors are also widely used in industry, particularly in the chemical industry, where they are employed to control the productive processes as well as to secure a safe working environment [2]. In addition, several studies have shown that measurements of certain gas concentrations in exhaled breath can aid the diagnosis of different diseases, for example, a high concentration of acetone can be linked to lung cancer [4].

Due to the heterogeneous and numerous applications where gas sensors are needed, a wide range of technologies have been developed through the years [5]. Among them, optical sensors have gained popularity because of their excellent features, such as robustness and resistance to harsh atmospheres, along with others [6]. In this context, optical sensors based on the Lossy Mode Resonance phenomenon (LMR) have attracted great attention in the last decade due to their good performance compared to state of the art optical sensors [7,8].

LMRs are generated when a thin film (with particular optical properties that will be later described) is deposited onto a waveguide. In these cases, some modes previously transmitted within the waveguide turn out to be guided through the thin film and, consequently, get attenuated. The attenuation occurs at a specific wavelength band, so an

absorption peak is obtained in the spectrum, known as LMR resonance. Different guided modes can experience the transition to the thin film, forming resonances of different orders. The LMR resonance has similar characteristic to the more mature Surface Plasmon Resonance [9], although the nature of the phenomenon is different.

Also, for each resonance, the transverse electric (TE) modes and transverse magnetic (TM) modes can generate different absorption peaks. In contrast SPRs only are generated in the TM mode. The LMR resonance wavelength is highly sensitive to the thickness and optical properties of the thin film as well as to the surrounding medium refractive index. Changes in these parameters produce a shift in the LMR resonance wavelength. The monitoring of this shift can be measured and it has been exploited in the fabrication of sensors for a wide variety of applications, such as oil degradation, humidity, pH, organic vapors, biosensing (Igg, D-dimer, gliadin), etc. [8].

The majority of LMR based sensors use optical fiber as the waveguide. Recently, planar waveguides (cover slips) based on lateral incidence of light, have started to gain popularity [10]. This setup avoids using an optical fiber, which is more brittle, or the Kretschmann configuration (used mainly in SPR-based sensors) [11], which is bulkier and presents difficulties to couple light at angles where LMRs are typically excited (near 90° with the normal of the surface where the thin-film is deposited) [10].

The LMR generating material (thin-film) must fulfill that the real part of the permittivity has to be positive and higher in magnitude than its own imaginary part and that of the material surrounding the thin film [12]. Metal oxides and polymers usually satisfy previous conditions. The number of LMR generating materials is wide and heterogeneous in comparison to those enabling the generation of the analogous phenomenon SPR [9] (mainly noble metals, such as gold and silver).

In this regard, graphene oxide (GO) has been found as an attracting LMR generating coating [13]. Its 2D nature, characterized by a high surface area, enables efficient interactions with target gas molecules, thereby enabling ultra-sensitive sensors [14]. Additionally, GO can be economically mass produced from graphite [15], making it an attractive option for sensor fabrication. Although there is still a long way to go to exploit its full potential as sensitive material, it is undoubtedly one of the most promising materials for gas sensing applications [16]. GO has already been employed in gas sensors with promising results [17]. In particular, GO based devices have been successfully used in electronic temperature and humidity sensors [18], as GO-DNA based sensors [19], or as optical fiber LMR-based sensor for the detection of ethanol in water [20], among others. An in-depth study of LMR-based gas sensors that compares different materials verifies that GO is a promising candidate for this type of sensors [7].

This work explores the combination of GO thin films deposited onto coverslips and the LMR sensing phenomenon for the fabrication of gas sensors. GO thin films have been fabricated onto planar waveguides by means of layer-by-layer (LbL) deposition technique. The sensitivity of the obtained devices to different gases (ethanol, vapor water and acetone) was studied. To the author´s knowledge this is the first time that GO is included in a planar LMR sensing device for gas detection.

2. Materials and Methods

2.1. Sensor fabrication

GO thin films were fabricated onto the waveguides using the LbL technique. Glass microscope coverslips from RS France, 18x18x0.15 mm made from soda lime glass were used as optical substrates and waveguides [21].

GO was purchased from Graphenea, S.A. (San Sebastian, Spain) and polyethylenimine (PEI) was obtained from Sigma-Aldrich. LbL fabrication of PEI/GO thin-films is explained in detail elsewhere [22]. A 0.5 mg/mL GO dispersion and 2 mg/mL PEI solution in DI water were prepared. PEI was left stirring overnight. GO dispersion was sonicated for 2 h before the deposition to enhance the dispersion of the GO nanosheets. The substrate

was cleaned with soap and water and dried with air prior to deposition. The surface of the substrate was activated by immersing it into a solution of KOH (1M) for 30min. The LbL deposition started with the immersion of the substrate into the PEI solution for 5 min. Then, the substrate was rinsed with DI water to remove the excess of material and dried in air for 1 min. Afterwards, the substrate was immersed into the GO dispersion for 5 min and subsequently rinsed in water and dried. The described routine formed the first bilayer of PEI/GO. The cycle was repeated multiple times for the deposition of more bilayers to increase the thickness of the film.

The surface homogeneity of the fabricated coating was characterized by means of a scanning electron microscope (FEI NanoSEM 450 FEG).

2.2. Optical setup

Fig 1 shows the optical transmission configuration for gas measurement. The setup consists of a Taki-MP halogen lamp (from PYROISTECH, Pamplona, Spain) as the excitation source, and a HR4000 VIS spectrometer (from OceanOptics Inc., Largo, FL, USA) for the monitoring of the LMR resonance wavelength shift. Two optical fibers were placed in contact with the facets of the coverslip to couple the light through the waveguide.

The sensor was tested with different concentrations of gases at a constant flow rate during measurements (200 mL/min). The chamber consisted of a sealed cylindrical cavity made of stainless steel with an inner diameter of 8.4 cm and height of 1.5 cm. A gas flow controller (EL-Mass flow Meters from Bronkhost®, Netherland) regulated the flow of the carrier gas (nitrogen N_2). N_2 gas was mixed with the gases under study (ethanol, water and acetone) that were evaporated using a Controller Evaporated Mixer (CEM) from Bronkhost®. The conduit between the chamber and the panel had a total length of 55 cm with an inner diameter of 5 mm. Due to the total system volume of the chamber (94 cm^3 including the conduit volume) and the selected flow rate, changes in the gas concentrations are not instantaneous. In fact, approximately 28 seconds are required to fully replace the gas inside the chamber.

The response and recovery times were estimated as the required time (when a new gas concentration is set) to go from 10 % to 90 % of the maximum wavelength shift value and vice versa.

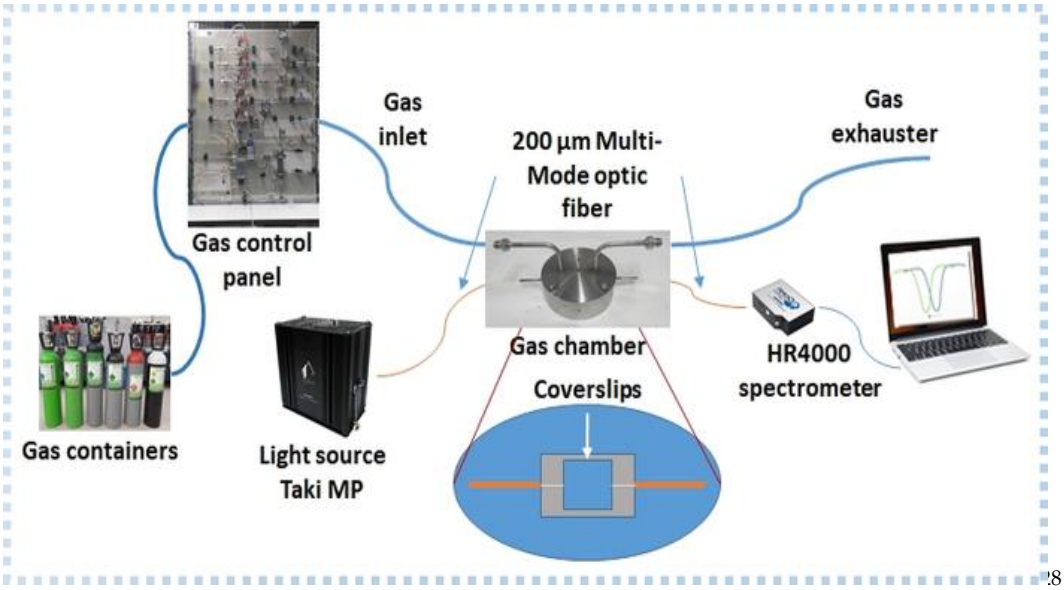

Figure 1. Gas measuring setup.

3. Results and discussion

Previous studies have shown the possibility to generate LMRs in optical fibers with PEI/GO thin films [20], however the generation of an LMR onto a planar waveguide, in

this case a coverslip, has not previously studied. In the present work, a resonance near 760 nm (resonance wavelength) was obtained after depositing 35 bilayers of PEI/GO. The number of bilayers exhibits a proportional relationship with the resonance wavelength (an increase in the number of bilayers results in a shift towards longer wavelengths [8]). In this study, 35 bilayers were selected to place the resonance within the region of the spectrum under examination (visible region).As it can be seen in Fig 2 b, the sensitive thin film is very uniform and homogeneous. In the SEM micrograph (Fig 2. c) it is possible to observe some wrinkles due to the folding of the GO nanosheets.

The resonance generated by this sensitive coating is wide compared to that generated by other materials [23]. Particularly, the width of the resonance between two points that are 0.1 dB higher than the center of the resonance is 501 nm (see Fig2. a) . This characteristic can be attributed to the structure of the GO sensing film, as the presence of a polymeric matrix with GO nanosheets results in a rough material. This characteristic was also observed with other coatings made of polymers and nanoparticles [24,25]. To consistently obtain the wavelength positions of the peaks at maximum absorbance, an algorithm that models absorbance spectral data with parabolic curves was created. Additionally, a sliding window algorithm was employed to reduce the noise.

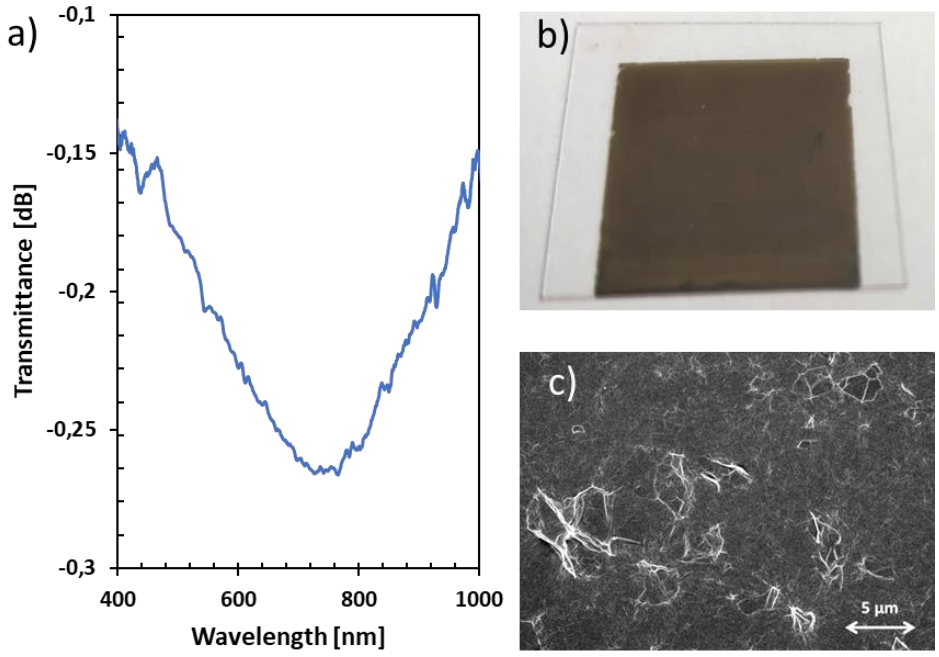

Figure 2. a) Transmittance spectra of the LMR with PEI/GO of 35 bilayers b) Coverslip coated with PEI/GO c) SEM micrograph of the PEI/GO thin film

Fabricated device was tested in a gas chamber with a mixture of N_2 and the previously mentioned evaporated gases at a constant flow of 200 mL/min. First, three cycles alternating a concentration of 0 and 50 mg/h of the selected gas were executed to check the repeatability of the measurements. Next, a few more cycles with different concentrations were performed to obtain the sensitivity of the device under test. Although the gas controllers are setup in mg/h, the concentrations of the gases are represented using more standard units (ppm in volume).

Wavelength resonance shifts associated with increasing concentrations of ethanol, acetone, and water vapor are shown in Figs. 3a), 3b) and 3c), respectively. It can be seen from Fig. 3 that the LMR shifts to higher wavelengths in all cases when increasing the gas concentration. The variations and noise presented when the LMR is stabilized at the different gas concentrations can be attributed to slight inaccuracies of the CEM that fix the

concentration of the gases. The shift of the LMR for ethanol was measured with concentrations between 600 and 1820 ppm (see Fig. 3 a). Lower ethanol concentrations could not be reached due to limitations in the gas flow controllers. The average ethanol response and recovery time were 123 s and 263 s respectively.

Acetone gas concentration was studied in the range between 3200 and 6390 ppm (see Fig. 3 b) obtaining an average response and recovery time of 187 s and 469 s respectively. The response to water vapor is showed in Fig. 3 c). In this case, the measured response and recovery time were 49 s and 696 s respectively. This fast response time can be attributed to the high capillary-like pressure in GO laminates [26].

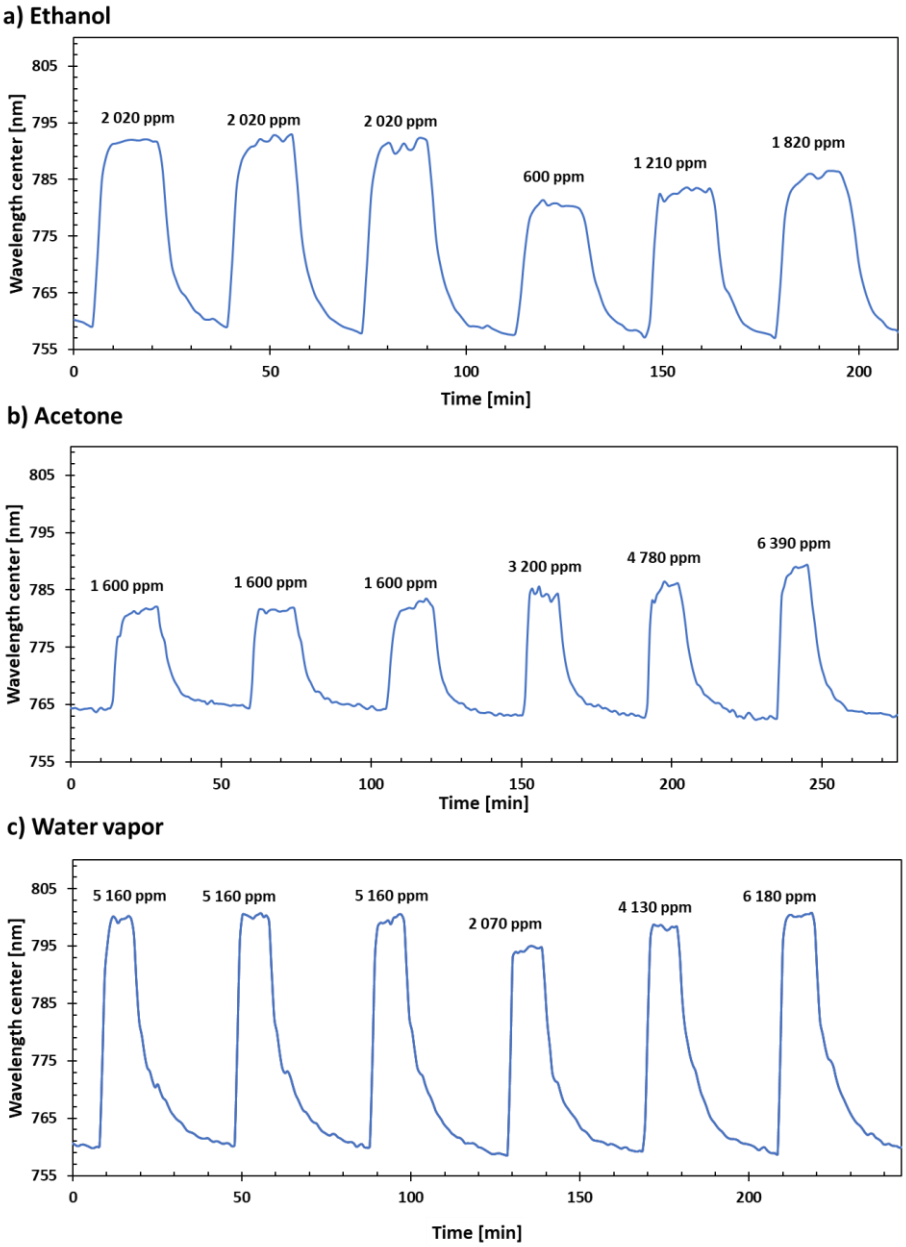

Figure 3. Dynamic response of the fabricated device to different concentrations of (a) ethanol, (b) acetone and (c) water vapor

The response of the device showed good repeatability to ethanol, acetone and water vapor for several cycles. The resonance wavelength shift versus gas concentration is represented in Fig. 4 to obtain the sensitivity of the sensor to the three selected gases. In the case of ethanol, the increase of the wavelength is linear to the concentration of the gas in the measured range (R^2=0.989), with a sensitivity of $4.826 \cdot 10^{-3}$ nm/ppm. The error bars represent the standard deviation of the measurements associated to inaccuracies of the CEM. The sensitivity of the device to acetone was remarkable inferior to that of ethanol (26.2% lower), with a sensitivity of $1.266 \cdot 10^{-3}$ nm/ppm and a R^2 value of 0.951. The sensitivity of the device to water vapor is $1.367 \cdot 10^{-3}$ nm/ppm with a linearity factor of R^2=0.989 in the studied range. In this case, the CEM evaporated water steadily, so the standard deviation is lower than that obtained with ethanol or acetone.

The combination of the linear response of the sensor and the high-resolution of the spectrometer (0.25 nm) allows the detection of small concentrations of the gases under study. Specifically in this work, the smallest variations that can be observed for ethanol, acetone and water vapor are 52, 197 and 183 ppm respectively. As shown in Fig 4, the trendlines do not intersect the origin of the axes, revealing a non-linear response of the device at lower gas concentrations (towards 0 ppm), which could lead to detect much smaller amounts using a more sophisticated equipment and more accurate gas controllers. In particular, ethanol detection shows promising results with the largest resonance shift (23 nm) at 600 ppm.

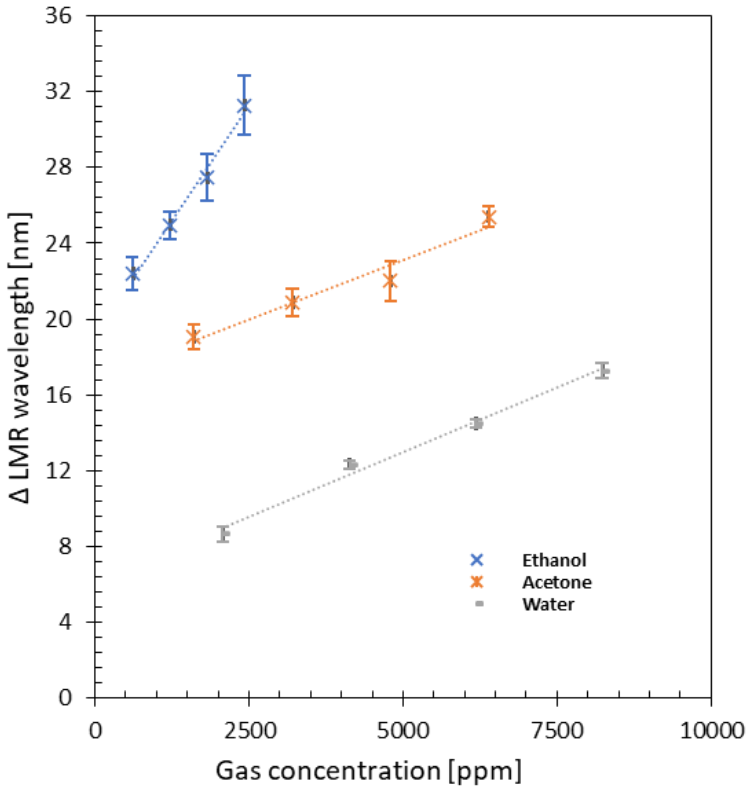

Figure 4. Sensitivity of the sensor, shift of the resonance, to different gas ethanol, acetone and water

The obtained parameters for each gas are summarized in Table 1. The sensitivity of the device to ethanol is ~3.5 times higher than the sensitivity to acetone and water vapor in the measured ranges. Moreover, the response time of the fabricated device to ethanol has the shortest recovery time. However, the best response time was obtained in the presence of water vapor, being 2 times shorter in comparison with the other two gases under study. This fact could be ascribed to the polarity of the gas molecules. In particular, the

relative polarity of selected gases is 0.654 for ethanol, 0.355 for acetone and it is specially high for water, 0.998 (normalized from measurements of solvent shifts of absorption spectra [27]). Therefore, the numerous functional groups present on the surface of GO particularly facilitate the intercalation of water molecules.

Table 1. Summarized response parameters of the sensor to different gases.

Gas	$[GAS]_{ppm}$	Sensitivity [nm/ppm]	Response time [s]	Recovery time [s]
Ethanol C_2H_5OH	600-2020	$4.826 \cdot 10^{-3}$	123	263
Acetone C_3H_6O	1600-6390	$1.266 \cdot 10^{-3}$	187	469
Water H_2O	2070-6180	$1.367 \cdot 10^{-3}$	49	696

The literature regarding LMR-based gas sensors utilizing GO is scarce. While there exist studies that investigate GO-based optical gas sensors, these often employ different phenomena, gas chambers, or waveguides, thus hindering direct comparison, particularly with regard to sensitivity. Table 2 presents an overview of the primary parameters of these investigations. It is worth noting that the detection limit of the studied sensor has not been fully established using the current gas setup and additional research is needed to achieve this goal and optimize the sensor's performance

Table 2. Summary of parameters for sensors with GO in the literature.

Gas	$[GAS]_{ppm}$	Detection limit	Waveguide	Phenomenon	Reference
(1) Ethanol (2) Acetone (3) Water	(1) 600-2020 (2) 1600-6390 (3) 2070-6180	-	Coverslip	LMR	Present work
Ethanol Ammonia Methanol	0-500	100 ppm*	Plastic optical fiber	Evanescent field	[28]
Ethanol	0-80	16 ppm*	Tapered polariztion-maintining fiber	Interferometer	[29]
(1) Ethanol (2) Acetone Others	(1) 164-823 (2)130-650	(1) 164 ppm* (2) 130 ppm*	Planar waveguide	Plasmonic nanospots	[30]
Ethanol Methanol	0-500	100 ppm*	Plastic optical fiber	Evanescent field	[31]
Humidity (Water)	-	30 % Relative humidity	Multimode optical fiber	LMR	[32]
Humidity (Water)	-	20 % Relative humidity	Type D single mode fiber	LMR	[33]

* Data not specified. The values are the minimum concentration found in the articles

3. Conclusions

A LMR based gas sensor was developed using GO as sensing material and a coverslip as waveguide. The probe was tested against ethanol, acetone and water vapor in a gas chamber with constant flow and utilizing an optical transmission setup. The device showed good repeatability and sensitivity to the three selected gases, especially in the case of ethanol ($4.826 \cdot 10^{-3}$ nm/ppm at room temperature). Sensitivities for water vapor and acetone were $1.367 \cdot 10^{-3}$ and $1.266 \cdot 10^{-3}$ nm/ppm respectively. Obtained device revealed high linearity in the studied range for the gases under test. This work shows a promising approach for the fabrication of gas sensors combining the utilization of GO and LMR-based sensing technology, as a preliminary step to attain highly sensitive devices and the advancement in the progress towards the commercialization of a lab-on-chip type sensor.

Acknowledgments: This work was supported by Agencia Estatal de Investigación (PID2019-106231RB-I00), Institute of Smart Cities and Public University of Navarra PhD Student grants, and in part by the European Union Horizon 2020 Research and Innovation Programme (Stardust-Holistic and Integrated Urban Model for Smart Cities) under Grant 774094. SM-E would like to express her gratitude for the Fellowship supported by the Royal Academy of Engineering under the Leverhulme Trust Research Fellowships scheme (LTRF2021\17130).

References

1. Ahmed Abdul–Wahab, S.A.; En, S.C.F.; Elkamel, A.; Ahmadi, L.; Yetilmezsoy, K. A review of standards and guidelines set by international bodies for the parameters of indoor air quality. *Atmos. Pollut. Res.* **2015**, *6*, 751–767, doi:10.5094/APR.2015.084.
2. Ghobakhloo, M. Industry 4.0, digitization, and opportunities for sustainability. *J. Clean. Prod.* **2020**, *252*, 119869, doi:10.1016/j.jclepro.2019.119869.
3. STARDUST project Available online: https://stardustproject.eu/.
4. Konvalina, G.; Haick, H. Sensors for Breath Testing : From Nanomaterials to Comprehensive Disease Detection. **2014**, *47*.
5. Liu, X.; Cheng, S.; Liu, H.; Hu, S.; Zhang, D.; Ning, H. A survey on gas sensing technology. *Sensors (Switzerland)* 2012.
6. Hodgkinson, J.; Tatam, R.P. Optical gas sensing: A review. *Meas. Sci. Technol.* **2013**, *24*, doi:10.1088/0957-0233/24/1/012004.
7. Vitoria, I.; Zamarreño, C.R.; Ozcariz, A.; Matias, I.R. Fiber optic gas sensors based on lossy mode resonances and sensing materials used therefor: A comprehensive review. *Sensors* **2021**, *21*, 1–26, doi:10.3390/s21030731.
8. Del Villar, I.; Arregui, F.J.; Zamarreño, C.R.; Corres, J.M.; Bariain, C.; Goicoechea, J.; Elosua, C.; Hernaez, M.; Rivero, P.J.; Socorro, A.B.; et al. Optical sensors based on lossy-mode resonances. *Sensors Actuators, B Chem.* **2017**, *240*, 174–185, doi:10.1016/j.snb.2016.08.126.
9. Tabassum, R.; Kant, R. Recent trends in surface plasmon resonance based fiber–optic gas sensors utilizing metal oxides and carbon nanomaterials as functional entities. *Sensors Actuators, B Chem.* **2020**, *310*, 127813, doi:10.1016/j.snb.2020.127813.
10. Fuentes, O.; Corres, J.M.; Matias, I.R.; Villar, I. Del Generation of Lossy Mode Resonances in Planar Waveguides Toward Development of Humidity Sensors. *J. Light. Technol.* **2019**, *37*, 2300–2306, doi:10.1109/JLT.2019.2902045.
11. Pandey, P.S.; Raghuwanshi, S.K.; Kumar, S. Recent advances in two-dimensional materials-based Kretschmann configuration for SPR sensors: A review. *IEEE Sens. J.* **2021**.
12. Del Villar, I.; Hernaez, M.; Zamarreno, C.R.; Sánchez, P.; Fernández-Valdivielso, C.; Arregui, F.J.; Matias, I.R. Design rules for lossy mode resonance based sensors. *Appl. Opt.* **2012**, *51*, 4298–4307, doi:10.1364/AO.51.004298.
13. Schöche, S.; Hong, N.; Khorasaninejad, M.; Ambrosio, A.; Orabona, E.; Maddalena, P.; Capasso, F. Applied Surface Science Optical properties of graphene oxide and reduced graphene oxide determined by spectroscopic ellipsometry. *Appl. Surf. Sci.* **2017**, *421*, 778–782, doi:10.1016/j.apsusc.2017.01.035.

14. Basu, S.; Bhattacharyya, P. Recent developments on graphene and graphene oxide based solid state gas sensors. *Sensors Actuators, B Chem.* **2012**, *173*, 1–21, doi:10.1016/j.snb.2012.07.092.
15. Hummers Jr, W.S.; Offeman, R.E. Preparation of graphitic oxide. *J. Am. Chem. Soc.* **1958**, *80*, 1339.
16. Tarcan, R.; Todor-Boer, O.; Petrovai, I.; Leordean, C.; Astilean, S.; Botiz, I. Reduced graphene oxide today. *J. Mater. Chem. C* **2020**, *8*, 1198–1224.
17. Toda, K.; Furue, R.; Hayami, S. Recent progress in applications of graphene oxide for gas sensing: A review. *Anal. Chim. Acta* **2015**, *878*, 43–53, doi:10.1016/j.aca.2015.02.002.
18. Borini, S.; White, R.; Wei, D.; Astley, M.; Haque, S.; Spigone, E.; Harris, N. Ultrafast graphene oxide humidity sensors. *ACS Nano* **2013**, 11166–11173.
19. Gao, L.; Lian, C.; Zhou, Y.; Yan, L.; Li, Q.; Zhang, C.; Chen, L.; Chen, K. Graphene oxide – DNA based sensors. *Biosens. Bioelectron.* **2014**, *60*, 22–29, doi:10.1016/j.bios.2014.03.039.
20. Hernaez, M.; Mayes, A.G.; Melendi-Espina, S. Graphene oxide in lossy mode resonance-based optical fiber sensors for ethanol detection. *Sensors (Switzerland)* **2018**, *18*, 1–10, doi:10.3390/s18010058.
21. Rubin, M. Optical properties of soda lime silica glasses m. rubin. **1985**, *12*, 275–288.
22. Kandjou, V.; Hernaez, M.; Acevedo, B.; Melendi-Espina, S. Interfacial crosslinked controlled thickness graphene oxide thin-films through dip-assisted layer-by-layer assembly means. *Prog. Org. Coatings* **2019**, *137*, 105345.
23. Fuentes, O.; Del Villar, I.; Corres, J.M.; Matias, I.R. Lossy mode resonance sensors based on lateral light incidence in nanocoated planar waveguides. *Sci. Rep.* **2019**, *9*, 1–10, doi:10.1038/s41598-019-45285-x.
24. Vitoria, I.; Coronel, C.; Ozcariz, A.; Zamarreño, C.R.; Matias, I.R. Lossy Mode Resonances Supported by Nanoparticle-Based Thin-Films. In *Sensing Technology*; Springer, 2022; pp. 135–147.
25. Hernaez, M.; Zamarreño, C.R.; Del Villar, I.; Matias, I.R.; Arregui, F.J. Lossy mode resonances supported by TiO2-coated optical fibers. *Procedia Eng.* **2010**, *5*, 1099–1102, doi:10.1016/j.proeng.2010.09.302.
26. Lian, B.; De Luca, S.; You, Y.; Alwarappan, S.; Yoshimura, M.; Sahajwalla, V.; Smith, S.C.; Leslie, G.; Joshi, R.K. Extraordinary water adsorption characteristics of graphene oxide. *Chem. Sci.* **2018**, *9*, 5106–5111.
27. Christian, R.; Thomas, W. Solvents and solvent effects in organic chemistry. *Wiley-VCH Publ. 3rd Ed. www. Org. org* **2003**, *15*, 2014.
28. Kavinkumar, T.; Sastikumar, D.; Manivannan, S. Effect of functional groups on dielectric, optical gas sensing properties of graphene oxide and reduced graphene oxide at room temperature. *RSC Adv.* **2015**, *5*, 10816–10825, doi:10.1039/c4ra12766h.
29. Jingle, Z.; Haiwei, F.; Jijun, D.; Min, Z.; Yi, Z. Graphene-oxide-coated interferometric optical microfiber ethanol vapor sensor. *Appl. Opt.* **2017**, *56*, 8828–8831.
30. Tabassum, S.; Wang, Q.; Wang, W.; Oren, S.; Ali, M.A.; Kumar, R.; Dong, L. Plasmonic crystal gas sensor incorporating graphene oxide for detection of volatile organic compounds. *Proc. IEEE Int. Conf. Micro Electro Mech. Syst.* **2016**, *2016-Febru*, 913–916, doi:10.1109/MEMSYS.2016.7421779.
31. Kavinkumar, T.; Sastikumar, D.; Manivannan, S. Reduced graphene oxide coated optical fiber for methanol and ethanol vapor detection at room temperature. *Optoelectron. Devices Integr. V* **2014**, *9270*, 92700U, doi:10.1117/12.2071841.
32. Hernaez, M.; Acevedo, B.; Mayes, A.G.; Melendi-Espina, S. High-performance optical fiber humidity sensor based on lossy mode resonance using a nanostructured polyethylenimine and graphene oxide coating. *Sensors Actuators, B Chem.* **2019**, *286*, 408–414, doi:10.1016/j.snb.2019.01.145.
33. Huang, Y.; Zhu, W.; Li, Z.; Chen, G.; Chen, L.; Zhou, J.; Lin, H.; Guan, J.; Fang, W.; Liu, X.; et al. High-performance fibre-optic humidity sensor based on a side-polished fibre wavelength selectively coupled with graphene oxide film. *Sensors Actuators, B Chem.* **2018**, *255*, 57–69, doi:10.1016/j.snb.2017.08.042.